



Article Info

Received: 15th December 2020Revised: 2nd February 2021Accepted: 4th February 2021

¹Department of Mathematics,
Sokoto State University, Sokoto,
Nigeria.

²Department of Mathematics,
Usmanu Danfodiyo University,
Sokoto, Nigeria

*Corresponding author's email:

abdulahihussaini6@gmail.com
Cite this: *CaJoST*, 2021, 1, 91-102

Radiation and Hall Effects on Magnetohydrodynamic (MHD) Free Convective Dissipative Fluid in the Presence of Heat Source

Hussaini Abdullahi^{1*} and Isah B. Yabo²

The investigation deals with a study of one dimensional free convective fluid flow through a porous medium due to combined effects of thermal and mass diffusion in the presence of n^{th} order chemical reaction. The objective of this work is to study heat and mass transfer in an unsteady MHD free convective flow past an infinite vertical plate with constant suction/injection. Energy equation takes into account of thermal radiation, heat source and Hall current effects. Dimensionless governing equations of the problem are solved numerically under appropriate transformed boundary conditions using an implicit finite difference scheme. Numerical solutions for temperature, velocity and concentration fields were obtained for suitable parameters such as buoyancy ratio parameter, Prandtl number, temperature dependent thermal conductivity and viscosity parameter, radiation parameter, Forchheimer parameter and Schmidt number. The local skin-friction, Nusselt number and Sherwood number were also presented and analyzed. The results obtained are discussed with the aid of graphs to observe impact of various parameters involved in the problem under investigation.

Keywords: Free convection, implicit finite difference scheme, variable viscosity, thermal conductivity, chemical reaction

1. Introduction

The investigation of free convection in a channel flow is significant because the analysis of such flows finds applications in cooling of electronic components of a nuclear reactor, designing ventilating and heat of buildings, bed thermal storage and heat sink in the turbine blades. Suneetha et al. [1] examined the interaction of radiation with mass transfer of a hydro magnetic, dissipative fluid in the presence of heat source/sink. They concluded that as radiation parameter increases, both the velocity and temperature increase, whereas the concentration decreases. Ibrahim et al. [2] researched on the problem of steady, laminar, free convection boundary layer flow of micro polar fluid from a vertical stretching surface embedded in a non-Darcian porous medium in the presence of thermal radiation, mass transfer, uniform magnetic field, heat generation, and free stream velocity using Runge-Kutta fourth order method with the shooting technique and predicted that micro polar fluids aids in the reduction of drag forces and also acts as agent of cooling. Awasthi [3] carried out investigation on the effects of heat and mass flux on MHD free convection flow through a porous medium with radiation and first order chemical reaction.

Interaction of radiation and heat source effects on MHD free convection flow over an inclined porous plate in the presence of viscous dissipation was studied by Omamoke et al. [4]. They observed that increasing magnetic field reduces the velocity profile, increases the temperature, skin friction and heat transfer profile. Melting and Radiation effects on MHD heat and mass transfer of Casson fluid flow past a permeable stretching sheet in the presence of Chemical reaction was emphasized by Ramana et al. [5]. "Melting and radiation effects on MHD heat and mass transfer of Casson fluid flow past a permeable stretching sheet in the presence of chemical reaction". A comprehensive scrutiny has been done on free convective heat and mass transfer flow through a highly porous medium with radiation, chemical reaction and Soret effects by Suneetha et al. [6]. Their results indicated that the velocity in the boundary layer increases with buoyancy parameters. A comprehensive analysis was conducted by Suneetha and Sailakumari [7] on the impact of thermal diffusion due to natural convection on MHD flow of a viscoelastic fluid past a porous plate with variable suction and heat source/sink is investigated by using a finite difference

technique. Suresh et al. [8] emphasized the impact of chemical reaction and radiation on MHD flow along a moving vertical porous plate with heat source and suction and numerically solved by the 4th-order Runge-Kutta method along with shooting technique.

Mahdy and Chamkha [9] examined Chemical reaction and viscous dissipation effects on Darcy-Forchheimer mixed convection in a fluid saturated porous media and solved numerically by employing the fourth-order Runge-Kutta integration scheme with Newton-Raphson shooting technique. A comprehensive analysis is presented to investigate the effects of thermophoresis on MHD Mixed convection, heat, and mass transfer about an isothermal vertical flat plate embedded in a fluid-saturated porous medium in the presence of viscous dissipation by [10]. Influence of viscous dissipation and radiation on the problem of Darcy-Forchheimer mixed convection from a vertical flat plate embedded in a fluid-saturated porous medium with thermal and mass diffusion was critically studied and reported by Salem [11]. Thermal dispersion effects on the Darcy-Forchheimer natural, mixed and forced convection heat transfer with viscous dissipation effects over an isothermal vertical flat plate in a fluid saturated porous media have been extensively examined numerically and reported by Nasser and Duwairi [12]. Majeed et al. [13] have designated Darcy-Forchheimer model with activation energy subject to chemically reactive species and momentum slip of order two and concluded that Sherwood number decreases in the presence of activation energy while opposite behavior is noticed for temperature difference ratio parameter. Sajid et al. [14] have deliberated magneto hydrodynamics (MHD) stretched flow of Maxwell Nano fluid with the convective boundary condition with consideration of some relevant physical parameters like activation energy, radiative heat flux and variable thermal conductivity. Beg et al. [15] have deliberated viscous, incompressible heat and mass transfer of a micro polar fluid through a non-Darcian porous medium in the presence buoyancy, Soret/Dufour diffusion, viscous heating and wall transpiration.

Quite a while ago, researchers assumed that both fluid viscosity and thermal conductivity were considered to be constant. Of late however, it is known that the physical properties of the fluid can be uttered significantly when exposed to temperature. For lubricants, heat generated by the internal friction and the ensuring rise in temperature affects both the viscosity and thermal conductivity and hence fluid viscosity and thermal conductivity are no longer assumed

to be fixed. This is true since in industrial system, fluid can be subjected to extreme conditions like high temperature, pressure, high shear rates and external heating and each of these mentioned can lead to high temperature being generated within the fluid. Extensive and in-depth reviews of the natural convection flows with variable viscosity and thermal conductivity have been presented by Animasaun [16], Kiran et al. [17], Babu et al. [18], Choudhury and Hazarika [19]. Swain et al. [20] have described steady two dimensional stagnation point flow of an incompressible conducting viscous fluid with variable properties over a stretching surface embedded in a saturated porous medium. This study inquire the essence of radiation and Hall Effect on Magnetohydrodynamic (MHD) free convective dissipative fluid in the presence of heat source with particular care to the variable viscosity, thermal conductivity and Forchheimer parameters in a vertical plate.

2. Mathematical Formulation

Consider the unsteady viscous temperature dependent heat mass transfer with n^{th} order chemical reaction over a vertical channel formed by two finite parallel plates separated by a distance H . The effects of uniform magnetic field, permeability, suction/injection, heat source, radiation, Soret and hall current effects are considered. From the onset, the temperature of the both vertical plates and the fluid are assumed to be T_h . At some time $t' > 0$, the temperature of the lower plate at $y' = 0$ rise to T'_ω . x' and y' are taken such that the flow is assume to be in the x' -direction, vertically upward along the channel walls and y' -axis normal to the plate. The physical configuration has been shown in Figure 1. Under the usual boundary layer and Boussinesq approximation and using the Darcy-Forchheimer model, the flow and heat transfer in the presence of radiation are governed by the following equations.

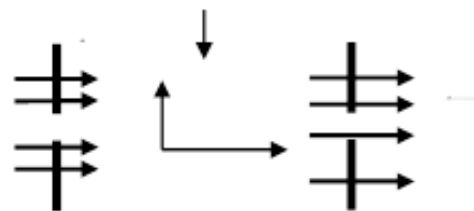


Figure1: Schematic diagram of the problem

Continuity equation

$$\frac{\partial v'}{\partial y'} = 0 \quad (1)$$

Momentum equation

$$\frac{\partial u'}{\partial t'} + v' \frac{\partial u'}{\partial y'} = \frac{\mu_0}{\rho} \frac{\partial}{\partial y'} \left\{ e^{-\lambda(T'-T_h)} \frac{\partial u'}{\partial y'} \right\} + g\beta(T'-T_h) + g\beta^*(C'-C_h) - \frac{\sigma B_0^2}{\rho} u' - \frac{\nu}{k'} u' - F'u'^2 \quad (2)$$

Heat transfer equation

$$\frac{\partial T'}{\partial t'} + v' \frac{\partial T'}{\partial y'} = \frac{k_0}{\rho c_p} \frac{\partial}{\partial y'} \left\{ [1+m(T'-T_h)] \frac{\partial T'}{\partial y'} \right\} - \frac{1}{\rho c_p} \frac{\partial q_r}{\partial y'} + \frac{\mu}{c_p} \left(\frac{\partial u'}{\partial y'} \right)^2 + \frac{Q_0}{\rho c_p} (T'-T_h) + b'u'^2 \quad (3)$$

Mass transfer equation

$$\frac{\partial C'}{\partial t'} + v' \frac{\partial C'}{\partial y'} = D \frac{\partial^2 C'}{\partial y'^2} - R(C'-C_h)^n + \sigma_1 \frac{\partial^2 T'}{\partial y'^2} \quad (4)$$

The corresponding initial and boundary conditions are prescribed as follows:

$$\begin{aligned} t' \leq 0: u' = 0, T' = T_h, C' = C_h \quad \text{for } 0 \leq y' \leq H \\ t' > 0: \begin{cases} u' = 0, T' = T_\omega, C' = C_\omega \quad \text{at } y' = 0 \\ u' = 0, T' = T_h, C' = C_h \quad \text{at } y' = H \end{cases} \quad (5) \end{aligned}$$

where u and v are the velocity components in x and y directions respectively, t' - the time, g - the acceleration due to gravity, β - the volumetric coefficient of thermal expansion, β^* - the volumetric coefficient of expansion with concentration, T' - the temperature of the fluid in the boundary layer, C' - the species concentration in the boundary layer, ν - the kinematic viscosity, σ - the electrical conductivity, B_0 - the magnetic induction, ρ - the density of the fluid, c_p - the specific heat at constant pressure, q_r - the radiation heat flux, Q_0 - the heat generation/absorption and D - the species diffusion coefficient, F^* - the Forchhiemer parameter, b^* - the Hall current parameter:

By use of Rosseland approximation value the radiative heat flux q_r is given by

$$q_r = -\frac{4\sigma^*}{3k^*} \frac{dT^4}{dy} \quad (6)$$

The present analysis is limited to optically thick fluids. If temperature differences within the flow are sufficiently small, then equation (6) can be linearized by expanding T^4 in Taylor series about T_h which after neglecting higher order terms takes the form.

$$T^4 = -3T_h^4 + 4T_h^3 T \quad (7)$$

Using equations (6) and (7), equation (3) simplifies to:

$$\frac{\partial T'}{\partial t'} + v' \frac{\partial T'}{\partial y'} = \frac{k_0}{\rho c_p} \frac{\partial}{\partial y'} \left\{ [1+m(T'-T_h)] \frac{\partial T'}{\partial y'} \right\} + \frac{1}{\rho c_p} \frac{16T_h^3 \sigma^*}{3k^*} \frac{\partial^2 T'}{\partial y'^2} + \frac{\mu}{c_p} \left(\frac{\partial u'}{\partial y'} \right)^2 + \frac{Q_0}{\rho c_p} (T'-T_h) + b'u'^2$$

The governing equations and the boundary conditions (1)-(5) are made non-dimensional, using the following non-dimensional variables.

$$x' = \frac{x}{H}, y' = \frac{y}{H}, t' = \frac{tH^2 Gr^{-1/2}}{\nu}, u' = \frac{uGr^{-1/2}}{\nu}, Gr = \frac{g\beta H^3 (T'_\omega - T_h)}{\nu^2}, \phi = \frac{Q_0 H^2}{\rho c_p \nu Gr^{1/2}},$$

$$T = \frac{T' - T_h}{T'_\omega - T_h}, C = \frac{C' - C_h}{C'_\omega - C_h}, Pr = \frac{\nu}{\alpha}, F = \frac{k_0 k}{4\sigma T_h^3}, Sc = \frac{\nu}{D}, Ec = \frac{u_0^2}{c_p (T'_\omega - T_h)}, N = \frac{\beta^* (C'_\omega - C_h)}{\beta (T'_\omega - T_h)}$$

$$M = \frac{\sigma B_0^2}{u_0^2}, Fr = \frac{F^* \nu}{T'_\omega - T_h}, b = \frac{b^* \nu}{u_0} \quad (9)$$

In view of equation (9), the equations (8), (2) and (4) reduce to

$$\frac{\partial u}{\partial t} + \eta \frac{\partial u}{\partial y} = \exp(-\lambda T) \left[\frac{\partial^2 u}{\partial y^2} - \lambda \frac{\partial u}{\partial y} \frac{\partial T}{\partial y} \right] + T + NC - \left(M + \frac{1}{Da Re} \right) u + F_1 u^2 \quad (10)$$

$$Pr \left[\frac{\partial T}{\partial t} + \eta \frac{\partial T}{\partial y} \right] = \left[1 + \gamma T + \frac{4}{3F} \right] \frac{\partial^2 T}{\partial y^2} + \gamma \left(\frac{\partial T}{\partial y} \right)^2 + Pr Ec \left(\frac{\partial u}{\partial y} \right)^2 + Pr \phi T + Pr b u^2 \quad (11)$$

$$Sc \left[\frac{\partial C}{\partial t} + \eta \frac{\partial C}{\partial y} \right] = \frac{\partial^2 C}{\partial y^2} - Sc Kr C^n + Sc Sr \frac{\partial^2 T}{\partial y^2} \quad (12)$$

Where η is the suction/injection parameter, γ is the thermal conductivity parameter, M is the magnetic parameter, F is the radiation parameter, Pr is the Prandtl number, Ec is the Eckert number, N is the buoyancy parameter, ϕ is the dimensionless heat generation/absorption coefficient, λ is the variable viscosity parameter and Sc is the Schmidt number, Fr is the inertia number, b is the Hall current.

The corresponding dimensionless boundary conditions are;

$$t > 0: \begin{cases} u = 0, & \theta = 1, C = 1 & \text{at } y = 0 \\ u = 0, & \theta = 0, C = 0 & \text{at } y = 1 \end{cases} \quad (13)$$

Numerical solutions

The governing equations (10) - (12) with the boundary conditions (13) are solved numerically using implicit finite difference scheme given by Makinde and Chinyoka (2011) and MALAB software. We used forward difference formulae for all time derivatives and approximate both the second and first derivatives with second order central differences to discretize the momentum, energy and concentration equations into finite difference equations. The equations are transformed into a system of linear algebraic equations in the tridiagonal form as:

$$-r_1 r_5 u_{i-1}^{j+1} + (1 + 2r_1 r_5) u_i^{j+1} - r_1 r_5 u_{i+1}^{j+1} = r_2 r_5 u_{i-1}^j + \left(1 + \eta r_4 - 2r_2 r_5 - \Delta t M - \frac{\Delta t}{Da Re}\right) u_i^j$$

$$+ (r_2 r_5 - \eta r_4) u_{i+1}^j + \Delta t Fr (u_i^j)^2 + \Delta t T_i^j + \Delta t NC_i^j \quad (14)$$

$$-r_1 r_6 T_{i-1}^{j+1} + (\text{Pr} + 2r_1 r_6) T_i^{j+1} - r_1 r_6 T_{i+1}^{j+1} = r_2 r_6 T_{i-1}^j + (\text{Pr} + 2r_2 r_6 + \eta r_4 \text{Pr} + \Delta t \text{Pr} \phi) T_i^j$$

$$+ (r_2 r_6 - \eta r_4 \text{Pr}) T_{i+1}^j + \gamma r_4 (T_i^j - T_{i-1}^j)^2 + r_4 \text{Pr} Ec (u_{i+1}^j - u_{i-1}^j)^2 + \Delta t \text{Pr} b (u_i^j)^2 \quad (15)$$

$$-r_1 C_{i-1}^{j+1} + (Sc + 2r_1) C_i^{j+1} - r_1 C_{i+1}^{j+1} = r_2 C_{i-1}^j + (Sc + \eta Sc r_4 - 2r_2) C_i^j - \Delta t Sc Kr (C_i^j)^q$$

$$+ (r_2 - \eta Sc r_4) C_{i+1}^j + r_7 (T_{i-1}^j - 2T_i^j + T_{i+1}^j) \quad (16)$$

Where

$$r_1 = \frac{\theta \Delta t}{\Delta y^2}, r_2 = \frac{(1-\theta)\Delta t}{\Delta y^2}, r_3 = \frac{\Delta t}{4\Delta y^2}, r_4 = \frac{\Delta t}{\Delta y}, r_5 = \exp(-\lambda T_i^j), r_6 = 1 + \gamma T_i^j + \frac{4}{3F}, r_7 = \frac{\Delta t Sc Sr}{\Delta y^2}.$$

θ is the weighing factor, and in implicit finite scheme the weighing factor θ is 1.

In each time step, firstly the concentration and temperature fields have been solved, then using the already known values of the concentration and temperature fields the velocity field is evaluated. The process of computation is advanced until a steady state is approached by satisfying the following convergence criterion.

$$\frac{\sum |A_{i,j+1} - A_{i,j}|}{M |A|_{\max}} < 10^{-5} \quad (17)$$

Here $A_{i,j}$ stands for the velocity or temperature fields, M is the number of interior grid points and $|A|_{\max}$ is the maximum absolute value of $A_{i,j}$. The expression for skin-friction, Nusselt number and Sherwood number are given as:

The skin-friction coefficient is given by

$$\tau = \left[\frac{\partial u}{\partial y} \right]_{y=0,1}$$

The Nusselt number is given by $Nu = \left[\frac{\partial T}{\partial y} \right]_{y=0,1}$

The Sherwood number is given by

$$Sh = \left[\frac{\partial C}{\partial y} \right]_{y=0,1}$$

3. Results and Discussion

The analysis of unsteady MHD free convective dissipative fluid flow past a vertical porous plate with variable viscosity, thermal conductivity in presence of heat source/ mass absorption, Hall current effect and suction/injection were conducted. The numerical solutions of the system of equations are analyzed for different values of the governing parameters and the results are presented graphically. The default values of the physical parameters are as follows: Radiation parameter (F), Reynolds number (Re), Magnetic field parameter (M), Heat generation/absorption parameter (ϕ), variable viscosity parameters (λ), variable thermal conductivity parameters (γ), Soret number (Sr) and Hall current effect parameter (b) are fixed as F=0.5, Re=0.01, M=10, ϕ =10.0, λ =1.0, γ =-0.5, Sr=1.0, b=0 for all the profiles except the varying parameter. Computations were performed for fluids with Prandtl number (Pr=0.71 and 7.0) corresponding to air and water respectively. The value of Schmidt number was taken as (Sc=0.22, 0.78, 0.94) representing diffusing chemical species of most common interest in air for hydrogen, ammonia and carbon dioxide. Hence all graphs correspond to these default values unless the varying parameters.

Figure 2 (a) and (b) displays the influence of buoyancy ratio parameter (N) on the dimensionless velocity for both air (Pr=0.71) and water (Pr=7.0) with respect to suction and injection. Buoyancy ratio parameter is the ratio of

thermal buoyancy force to mass buoyancy force. The Figures depict that velocity gets accelerated on increasing buoyancy ratio parameter (N) for ($N > 0$) since both thermal buoyancy force and mass buoyancy force move in same direction. On the other hand, velocity decreases on increasing buoyancy ratio parameter ($N < 0$). It is due to the reason that mass buoyancy force act opposite to thermal buoyancy force.

Figure 3 (a) and (b) emphasize the impact of magnetic field (M) on fluid velocity for both air ($Pr=0.71$) and water ($Pr=7.0$) as working fluid under the influence of suction and injection. It is concluded from Figures that velocity (u) decreases in the region near the plate on increasing magnetic field parameter (M) while it increases in the region away from the plate on increasing magnetic parameter (M). This implies that magnetic field tends to retard fluid velocity in the region near the plate whereas it has a reverse effect on fluid velocity in the region away from the plate. This is due to the Lorentz forces which have to act against the flow.

Variations of the velocity curve is shown in Figure 4 (a) which illustrates that the velocity decreases with increase of Prandtl number ($Pr=0.71, 3.0$ and 7.0). This is because Prandtl number is the ratio of momentum diffusion to thermal diffusion in the boundary layer regime. For $Pr=1.0$, the momentum diffusion rate is greater than thermal diffusion rate, therefore the velocity in the fluid regime will decreased with rise in Pr . Also, it observed from Figure 3 (b), that the temperature profile decreases as the Prandtl number ($Pr=0.71, 3.0$ and 7.0) increases due to the decrease in the fluid thermal diffusivity. This is so because at higher Prandtl number, the fluid has thinner thermal boundary layer and this enhances the slop of the temperature profile.

The influence of variable thermal conductivity parameter (γ) on the velocity and temperature profiles is illustrated in Figures 5 (a) and (b). While all other participating parameters in both fields are held fixed and variable thermal conductivity parameter (γ) is increase, a drop in velocity is shown as depicted in Figure 5 (a). It is further noticed that as variable thermal conductivity parameter (γ) increases the temperature field enhances as displayed in Figure 5 (b).

Figures 6 (a) and (b) exhibit the effects of Schmidt number (Sc) on dimensionless velocity and concentration. It is noticed from Figure 6 (a) that, fluid velocity retards on increasing Sc . Schmidt number refers to the ratio of momentum diffusivity to mass diffusivity. This shows that

mass diffusion tends to accelerate the fluid flow in the boundary layer region. Figure 6 (b) highlights the effect of Schmidt number (Sc) on dimensionless concentration. It declares that the concentration distribution decreases at all points of the flow field with the increase of the Schmidt number. The Schmidt number embodies the ratio of the momentum diffusivity to the mass diffusivity. The Schmidt number therefore quantifies the relative effectiveness of momentum and mass transport by diffusion in the velocity and concentration boundary layers. As the Schmidt number increases the concentration decreases.

The variation of Soret number (Sr) on the velocity and concentration profiles are presented in Figures 7 (a) and (b) with suction and injection. From Figure 7 (a) we realize that velocity profiles enhance with an increasing of Soret number (Sr). This is true, since fluid velocity rises due to thermal diffusion. It is further, noticed from Figure 7 (b) as we vary the values of Soret number (Sr), the concentration profiles is significantly increase.

Figures 8 (a) and (b) highlight the variation of velocity and temperature profiles for different values of radiation parameter (F). Here, we observed that as the value of F increases both the velocity and temperature increases with an increasing in the flow boundary layer thickness, hence thermal radiation accelerate convective flow.

The influence of variable viscosity parameter (λ) is emphasized in Figures 9 (a) and (b) by considering different values of the parameter. The Figures report that as the variable viscosity parameter (λ) increases the velocity enhances. It is further acknowledged from the Figures that, velocity is higher in air ($Pr=0.71$) compared to that of water ($Pr=7.0$) for both suction and injection.

Figures 10 (a) and (b) demonstrate the impact of chemical reaction (Kr) on dimensionless velocity and concentration profiles. It is reported from Figure 9 (a) that fluid velocity decreases on increasing chemical reaction parameter (Kr). It is also from Figure 10 (b), reveals the variation of chemical reaction parameter (Kr) on dimensionless concentration profiles. It concludes that concentration decreases with the increase of chemical reaction parameter. Since chemical reaction parameter has a retarding influence on the concentration distribution of the flow field.

Figures 11 (a) and (b) exhibits the behavior of dimensionless velocity profiles for various values

of Darcy Forchhiemer parameter (Fr) with respect to suction and injection. It is reported from the Figures that increasing Darcy Forchhiemer parameter (Fr) decelerates the velocity in both suction and injection. Also, it is detected velocity is higher in air (Pr= 0.71) compared to water (Pr=7.0).

and (b). While all other participating parameters in the field are held fixed and Hall current parameter (b) is increase, a drop in velocity is shown as depicted in Figure 4 (a) and (b). It is further noticed that increasing Hall current parameter (b) enhances the gradient of the temperature profile in water (Pr=7.0) as compared in air (Pr=0.71) in both suction and injection as seen in the Figures.

The influence of Hall current parameter (b) on the velocity profiles is illustrated in Figure 12 (a)

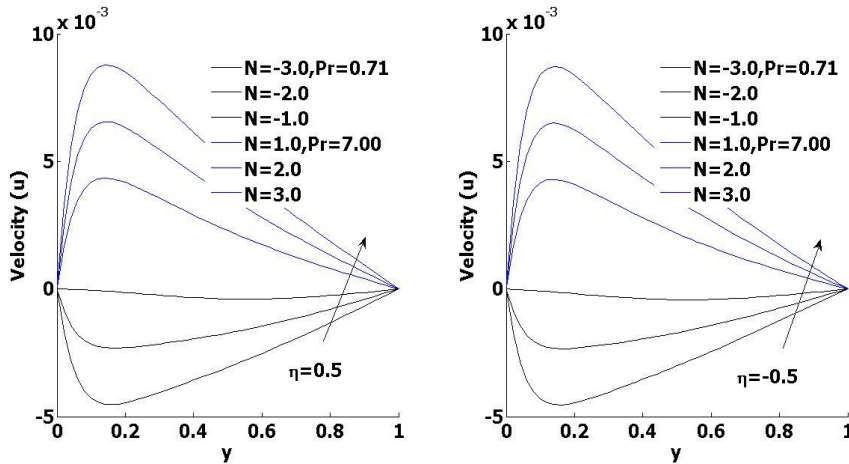


Figure 2 (a) and (b): Effect of buoyancy ratio parameter (N) on velocity profiles.

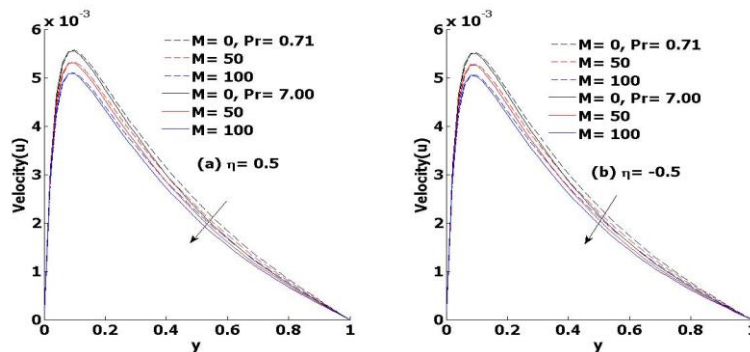


Figure 3 (a) and (b): Effect of magnetic parameter (M) on velocity profiles.

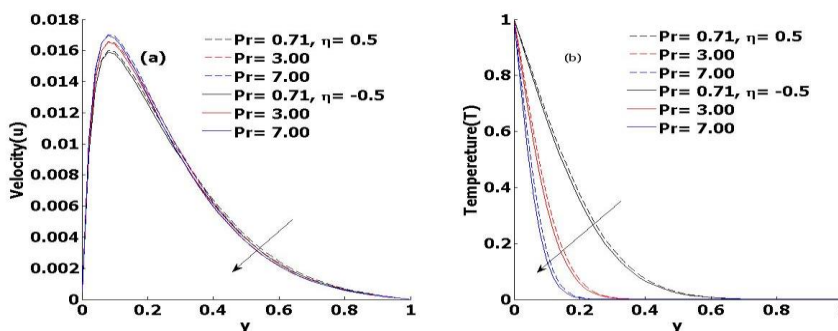


Figure 4 (a) and (b): Effect of Prandtl number (Pr) on velocity and temperature profiles.

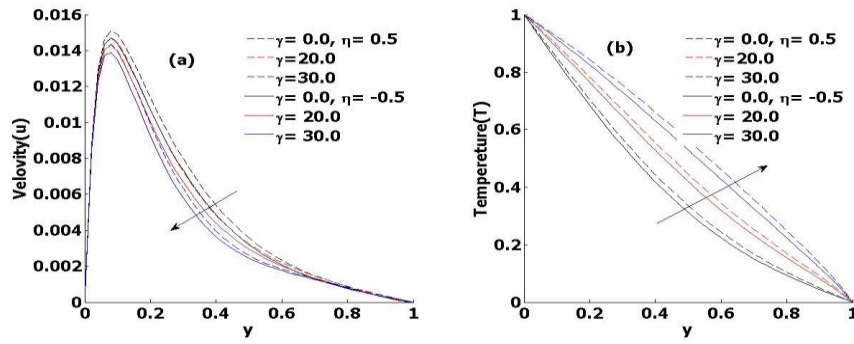


Figure 5 (a) and (b): Effect of thermal conductivity parameter (γ) on velocity and temperature profiles

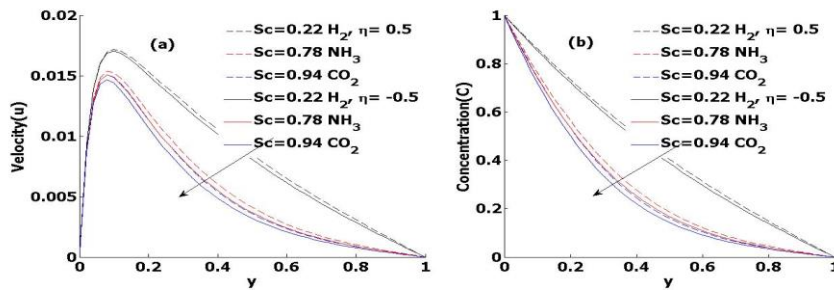


Figure 6 (a) and (b): Effect of Schmidt number (Sc) on velocity and concentration profiles.

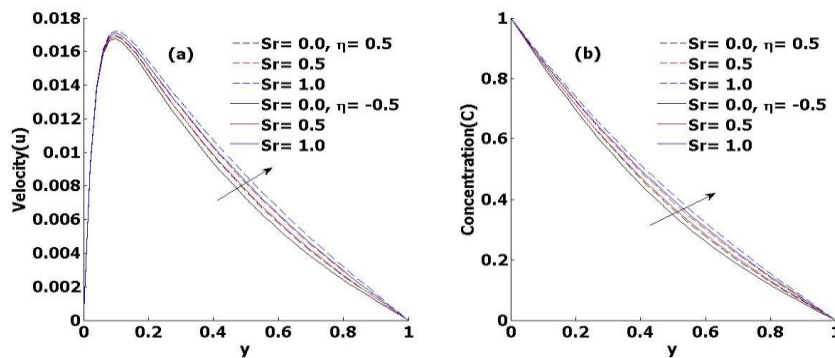


Figure 7 (a) and (b): Effect of Soret number (Sr) on velocity and concentration profiles.

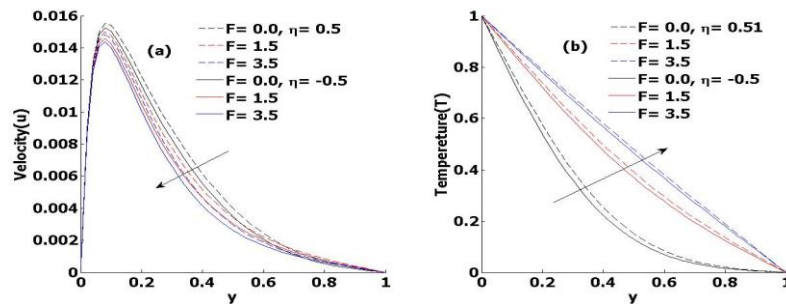


Figure 8 (a) and (b): Effect of radiation parameter (F) on velocity and temperature profile.

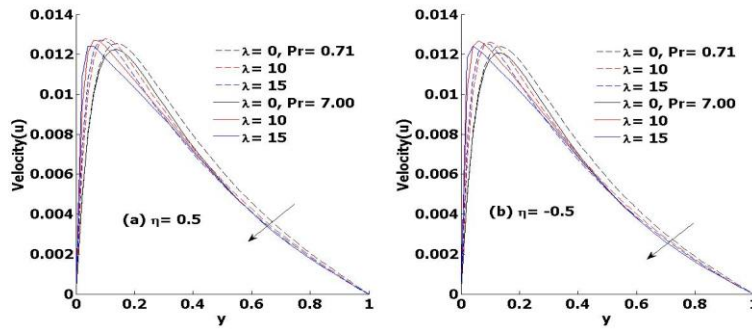


Figure 9 (a) and (b): Effect of variable viscosity parameter (λ) on velocity profiles.

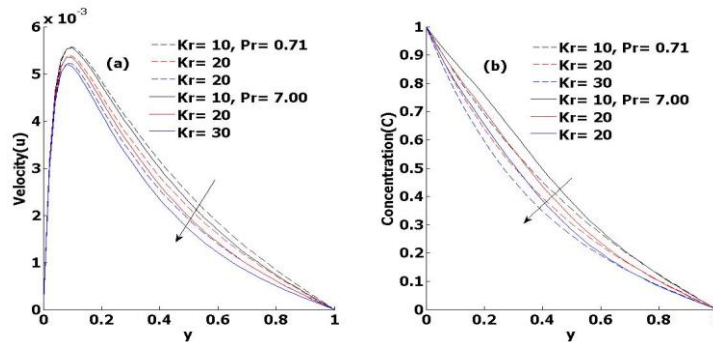


Figure 10 (a) and (b): Effect of chemical reaction parameter (Kr) on velocity and concentration.

Profiles

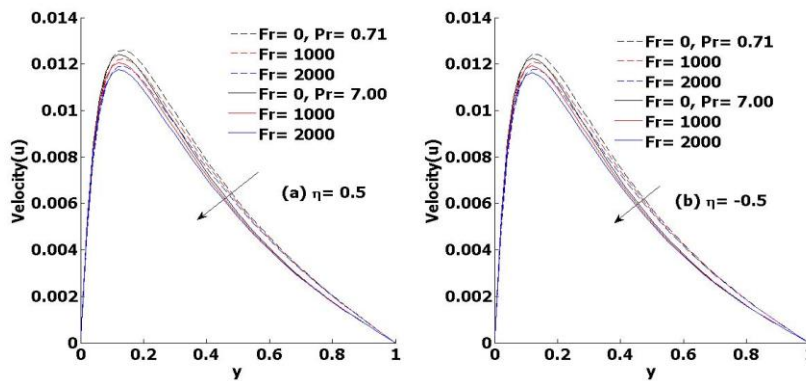


Figure 11 (a) and (b): Effect of Forchhiemer parameter (Fr) on velocity profiles.

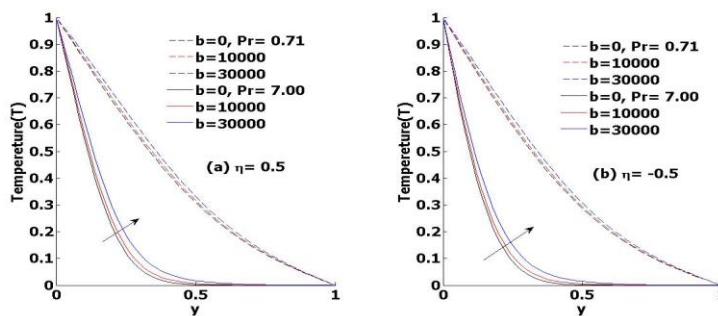


Figure 12 (a) and (b): Effect of Hall current parameter (b) on temperature profiles.

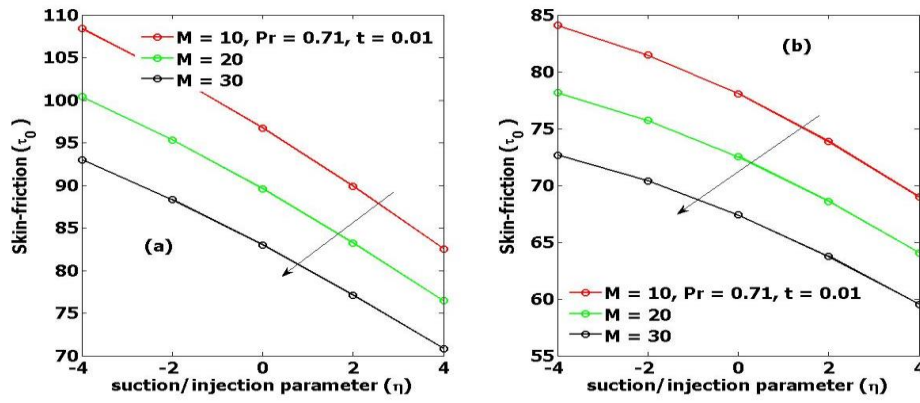


Figure 13 (a) and (b): Skin friction against M at $y=0$.

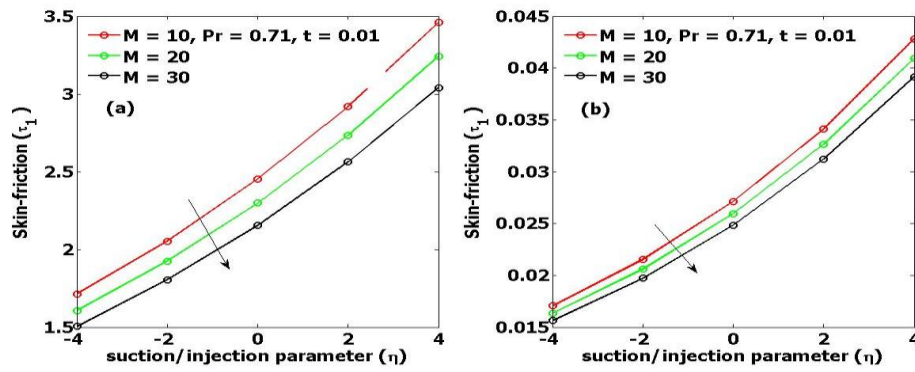


Figure 14 (a) and (b): Skin friction against M at $y=1$.

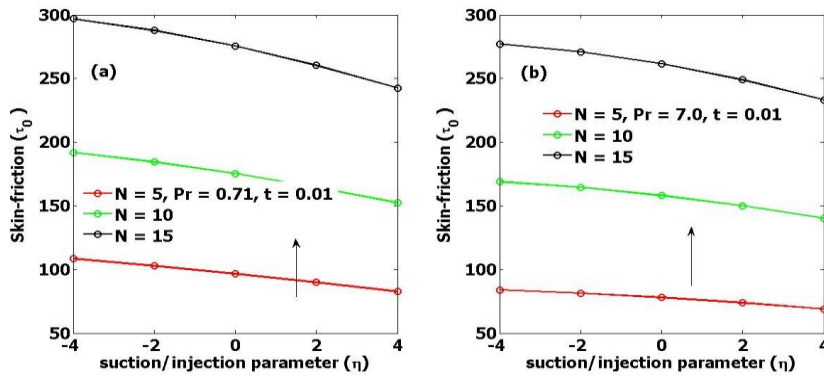


Figure 15 (a) and (b): Skin friction against N at $y=0$

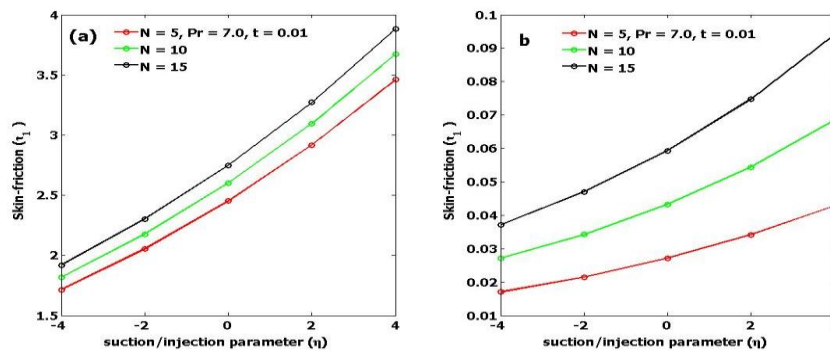


Figure 16 (a) and (b): Skin friction against N at $y=1$

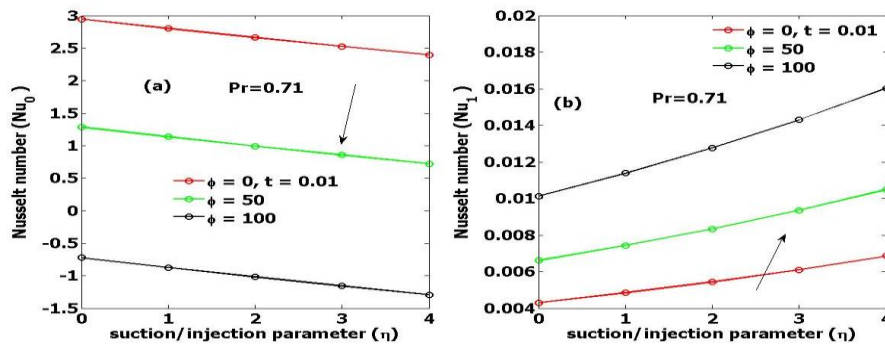


Figure 17 (a) and (b): Nusselt number against ϕ at $y=0$ and at $y=1$

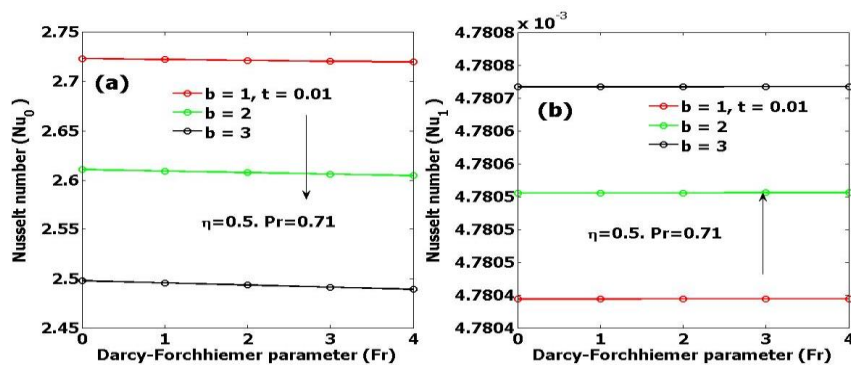


Figure 18 (a) and (b): Nusselt number against ϕ at $y=0$ and at $y=1$

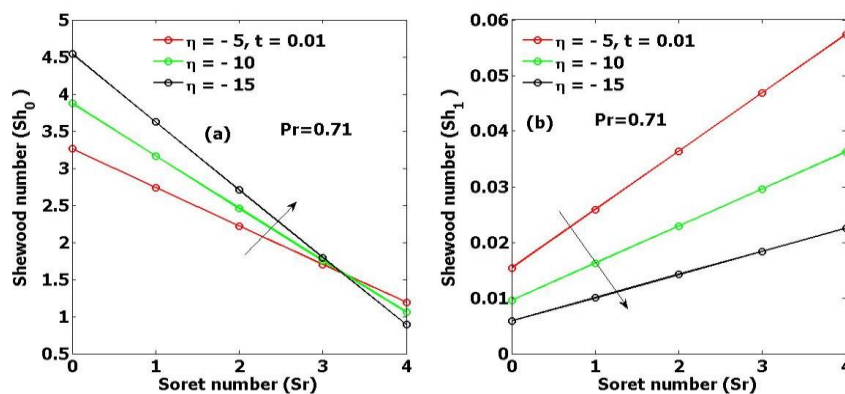


Figure 19 (a) and (b): Sherwood number against η at $y=0$ and at $y=1$

The impact of magnetic parameter (M) with reference to suction/injection parameter (η) is highlighted in Figure 13 (a) and (b) and Figure 14 (a) and (b) for the boundary surface $y=0$ and $y=1$ respectively. It is reported from the Figures that as the magnetic parameter (M) increases, the skin friction is noticed to be decreasing at the plate $y=0$ and $y=1$. Also, when the magnetic parameter is held constant and as suction/injection parameter increases, the skin friction reduces at the boundary surface $y=0$ and increases at the boundary surface $y=1$ as depicted in the Figures. The variation of buoyancy parameter (N) with respect to the suction/injection parameter (η) on skin friction is

illustrated in Figure 15 (a) and (b) through Figure 16 (a) and (b). It is emphasized that, as the buoyancy parameter (N) increases, the skin friction on the boundary surfaces $y=0$ and $y=1$ increases. It is also realized that, suction/injection parameter (η) increases, keeping the buoyancy parameter (N) fixed, the skin friction the plate $y=0$ shrinks and enhances the plate $y=1$ as indicated in the Figures.

The effect of heat generation/absorption parameter (ϕ) on Nusselt number is demonstrated in Figure 17 (a) and (b). It is declared that as the heat generation/absorption parameter (ϕ) increases the Nusselt number

decreases at the boundary surface $y=0$ and accelerates at the boundary surface $y=1$ as seen in the Figures. The Figures further informed that as suction/injection parameter (η) increases, the Nusselt number decelerates at the plate $y=0$ and accelerates at the plate $y=1$. Variation of Hall current parameter (b) with respect to Darcy-Forchheimer parameter (Fr) is observed in Figure 18 (a) and (b). It is noticed in Figure 18 (a) that as the Hall current parameter (b) increases the Nusselt number on the boundary surface $y=0$ decreases and increases on the boundary surface $y=1$. It is also reported from the Figures that, as the Darcy-Forchheimer parameter (Fr) increases with respect to Hall current parameter (b), not much significant change is seen.

Figure 19 (a) and (b) exhibits the effect of suction/injection parameter (η) on Sherwood number with reference to Soret number (Sr). It is pointed out that as the suction/injection parameter (η) varies, the Sherwood number decreases at the boundary $y=0$ and increases at the boundary $y=1$ as highlighted in Figure 19 (a) and (b). It is further concluded from the figures that, when suction/injection parameter (η) is held constant and as Soret number (Sr) increases, the Sherwood number decreases at the boundary surface $y=0$ and accelerates at the boundary surface $y=1$.

4. Conclusion

An analysis was carried out for free convective flow and heat transfer of a reacting flow over a vertical plate in the presence of variable viscosity, thermal conductivity and Hall current effects. The governing equations for the velocity field, temperature and concentration was solved by perturbation technique in terms of dimensionless parameters. The findings of this study are as follows:

1. Velocity increase as buoyancy ratio (N), Soret number (Sr), are increases and Velocity decrease in case of magnetic parameter (M), Prandtl number (Pr), variable thermal conductivity parameter (γ), Schmidt number (Sc), thermal radiation parameter (F), variable viscosity parameter (λ), chemical reaction parameter (Kr) and Forchheimer parameter (Fr).
2. Temperature decrease as Pr increase, however increase in the case of variable thermal conductivity parameter (γ), thermal radiation parameter (F) and Hall current parameter.

3. The Concentration retards with an increase in Sc , Kr but accelerates in the case of Sr .
4. Skin friction increases with an increase of buoyancy ratio parameter (N) but a reverse effect is noticed in the case of magnetic parameter (M) and suction/injection (η).
5. Nusselt number decreases as heat generation parameter (ϕ) increases but in the case of suction/injection parameter (η) it decreases with increasing suction/injection parameter (η) at the boundary surface $y=0$ but the reverse effect is reported on the boundary surface $y=1$.

Conflict of interest

The authors declare no conflict of interest.

References

- S. Suneetha, N. Bhaskar Reddy, Ramachandra Prasad (2011). Radiation and Mass Transfer Effects on MHD Free Convective Dissipative Fluid in the Presence of Heat Source/Sink. *Journal of Applied Fluid Mechanics*, **4**(1), 107-113.
- S. Mohammed Ibrahim, T. Shankar Reddy, and N. Bhaskar Reddy (2013). "Radiation and Mass Transfer Effects on MHD Free Convection Flow of a Micro polar Fluid past a Stretching Surface Embedded in a Non-Darcian Porous Medium with Heat Generation" *Thermodynamics*, Volume 2013, Article ID 534750, 15pages.
- B. Awasthi (2018). "Effects of Heat and Mass flux on MHD free convection flow through a porous medium with radiation and first order chemical reaction". *Int. J. of Applied Mechanics and Engineering*, **23**(4), 855-871.
- Ekakitie Omamoke, Emeka Amos, Kubugha Wilcox Bunonyo (2020). "Radiation and Heat Source Effects on MHD Free Convection Flow over an Inclined Porous Plate in the Presence of Viscous Dissipation". *American Journal of Applied Mathematics*. **8**, (4), 190-206.
- R. Mohana Ramana, J. Girish Kumar, and K. Venkateswara Raju (2020): AIP Conference Proceedings 2246, 020021 (2020); <https://doi.org/10.1063/5.0014732>.
- K. Suneetha, S Mohammed Ibrahim and G V Ramana Reddy, "A Study on free convective heat and mass transfer flow through a highly porous medium with radiation, chemical reaction and Soret effects" *Journal of*

- Computational and Applied Research in Mechanical Engineering*, Vol. 8, No. 2, pp. 121-132, (2019).
- T. Suneetha, A. Sailakumari, "Heat and Mass Transfer Characteristics of MHD Free Convective Rivlin-Ericksen Fluid Flow Past a Porous Plate." *International Journal of Mathematics Trends and Technology* (IJMTT) – Vol. 53 No. 6, pp. 441-452, (2018).
- P. Suresh, Y. Hari Krishna, R. Sreedhar Rao, P. V. Janardhana Reddy. "Effect of chemical reaction and radiation on MHD Flow along a moving vertical porous plate with heat source and suction". *International Journal of Applied Engineering Research*, Vol. 14, No. 4 (2019) pp. 869-876.
- A. Mahdy, A.J. Chamkha, "Chemical reaction and viscous dissipation effects on Darcy-Forchheimer mixed convection in a fluid saturated porous media". *International Journal of Numerical Methods for Heat & Fluid Flow* Vol. 20 No. 8, 2010, pp. 924-940.
- N. Kishan, Srinivas Maripala, "Thermophoresis and viscous dissipation effects on Darcy-Forchheimer MHD mixed convection in a fluid saturated porous media". *Advances in Applied Science Research*, 2012, 3 (1):60-74.
- A. M. Salem "Coupled Heat and Mass Transfer in Darcy-Forchheimer Mixed Convection from a Vertical Flat Plate Embedded in a Fluid-Saturated Porous Medium under the Effects of Radiation and Viscous Dissipation". *Journal of the Korean Physical Society*, Vol. 48, No. 3, March 2006, pp. 409-413.
- Ibrahim Nasser and, H. M. Duwairi, "Thermal Dispersion Effects on Convection Heat Transfer in Porous Media with Viscous Dissipation". *International Journal of Heat and Technology*, Vol. 34, No. 2, 2016, pp. 207-212, DOI: 10.18280/ijht.340208.
- A. Majeed, A. Zee Shan, and F. M. Noori, "Numerical study of Darcy-Forchheimer model with activation energy subject to chemically reactive species and momentum slip of order two". *AIP Advances* 9, 045035 (2019); doi: 10.1063/1.5095546 9, 045035-1.
- T. Sajid, M. Sagheer, S. Hussain, and M. Bilal, "Darcy-Forchheimer flow of Maxwell Nano fluid flow with nonlinear thermal radiation and activation energy". *AIP Advances* 8, 035102 (2018); <https://doi.org/10.1063/1.5019218>.
- O.A. Bé, R. Bhargava, S. Rawat, E. Kahya, "Numerical Study of Micro polar Convective Heat and Mass Transfer in a Non-Darcy Porous Regime with Soret and Dufour diffusion Effects, *Emirates Journal for Engineering Research*, 13 (2), 51-66 (2008).
- I.L. Animasaun, "Effects of thermophoresis, variable viscosity and thermal conductivity on free convective heat and mass transfer of non-Darcian MHD dissipative Casson fluid flow with suction and nth order of chemical reaction", *Journal of the Nigerian Mathematical Society* 34 (2015) 11–31.
- Kiran Kumar, G., Srinivas, G., Babu, S., & Srikanth, G. (2018). "Effects of Variable Viscosity and Thermal Conductivity on MHD Convective Heat Transfer of Immiscible Fluids in a Vertical Channel, *International Journal of Engineering Sciences & Research Technology*, 7(5), 73-73-79.
- S.R. Ravi Chandra Babu, S. Venkateswarlu, K. Jaya Lakshmi, "Effect of Variable Viscosity and Thermal Conductivity on Heat and Mass Transfer Flow of Nano fluid over a Vertical Cone with Chemical Reaction", *International Journal of Applied Engineering Research* Vol. 13, No. 18 (2018) pp. 13989-14002.
- M. Choudhury, and G. C. Hazarika, "The Effects of Variable Viscosity and Thermal Conductivity on MHD Oscillatory Free Convective Flow past a Vertical Plate in Slip Flow Regime with Variable Suction and Periodic Plate Temperature, *Journal of Applied Fluid Mechanics*, Vol. 6, No. 2, pp. 277-283, 2013.
- K. Swain, S.K. Parida, G.C. Dash, "MHD Heat and Mass Transfer on Stretching Sheet with Variable Fluid Properties in Porous Medium", *AMSE JOURNALS-AMSE IIETA publication-2017-Series: Modelling B*; Vol. 86; No 3; pp. 706-726.